

# OBSERVER-BASED FLUX ESTIMATION MODELS IMPLEMENTATION FOR DIRECT FIELD ORIENTED CONTROL OF INDUCTION MACHINE DRIVES

Aitor J. Garrido  
Departamento Ingeniería de  
Sistemas y Automática  
E.U.I.T.I. Bilbao  
Plaza de la Casilla  
48012 Bilbao (Spain)  
University of the Basque  
Country

Francisco J. Maseda  
Departamento Ingeniería de  
Sistemas y Automática  
E.U.I.T.I. Bilbao  
Plaza de la Casilla  
48012 Bilbao (Spain)  
University of the Basque  
Country

Oscar Barambones  
Departamento Ingeniería de  
Sistemas y Automática  
E.U.I.T.I. Bilbao  
Plaza de la Casilla  
48012 Bilbao (Spain)  
University of the Basque  
Country

M. De la Sen  
Instituto de Investigación y  
Desarrollo de Procesos-IIDP  
Fac. de Ciencia y Tecnología  
48080 Bilbao (Spain)  
University of the Basque  
Country  
<http://www.ehu.es/IIDP>

E

## ABSTRACT

In this paper two different observed-based flux estimation models to be used in the DFO control of induction machines are presented. The main idea relies on the use of estimation rather than direct measurement of the air gap flux, avoiding the inconveniences associated to the need of intrusive sensors. It is provided a performance analysis and comparison of both flux observers when applied to the speed tracking problem of a piecewise loaded induction motor drive in a wide speed operation range, perusing their behaviour in order to profit the advantages of each one in a combined way.

## KEY WORDS

Modelling, Power Systems, Vector Control, Induction Machine Drives, Simulation.

## 1. Introduction

As it is well known, field oriented or vector control is used to deal with the torque and flux coupling effect inherent to ac drives that can not be avoided using other kind of scalar controls, providing a dc-machine-like and fast transient response (see for instance [1], [2] and [3]). In this sense, field oriented control has been established as the industrial standard high performance control method for induction machine drives (IMD).

There are two general techniques of vector control; Indirect Field Orientation (IFO) consist of a feedforward scheme that makes the process highly sensitive to parameter uncertainties and load disturbances (see [4], [1]), specially in large and high-efficiency machines operating in field weakening conditions (see [5]). So, it is usual to utilize this method jointly with a parameter adaptation scheme (see [6], [7] and [8]). And Direct Field Orientation (DFO), which is based on the direct measurement or estimation of either the rotor or stator flux (see [9] and [1]). Nevertheless, rotor flux provides a

natural decoupling if using a convenient orientation, an it is so, more interesting. The direct measurement of the air gap flux presents the inconveniences of the lack of mechanical robustness and behaviour associated to the need of intrusive sensors. On the other hand, flux angle measurement using phase voltage saturation-induced third harmonic methods introduces complexity and does not eliminates the use of sensors to quantify the rotor flux magnitude (see [10] and [11]). Therefore, the use of estimation rather than measurement of the rotor flux for direct field orientation stands as one of the most interesting techniques for the vector control of induction machine drives.

In particular, this paper presents two different observed-based flux estimation models to be implemented in a DFO control scheme, providing a performance analysis and comparison when applied to the speed tracking problem of a piecewise loaded induction motor drive.

The paper is organized as follows. Section 2 provides some background on Vector Control focusing on observed-based DFO Control. In Sections 3 and 4, the proposed current-based and voltage-based flux observers are developed, respectively. Section 5 presents two different simulation examples and finally, concluding remarks are stated in Section 6.

## 2. Background on DFO Control

DFO control is a feedback method consisting of obtaining the principal command vector control parameters  $i_{ds}^{e*}$  and  $i_{qs}^{e*}$ , that is, the stator current torque and flux components referred to a rotating reference frame, from estimates of the rotor flux. This rotating reference frame moves synchronously with the rotor, allowing the manipulation of the flux and torque separately and in a decoupled manner. To do so, two reference frame transformations are needed; The first one to transform the three-phase

reference frame variables ( $a-b-c$ ) into a two-phase stationary reference frame variables ( $d^e-q^e$ ). And the second one to transform these to the synchronously rotating reference frame ( $d^e-q^e$ ) as explained below.

## 2.1. Background on Field Orientation of IMD

The mechanical equation of an induction motor drive can be written as:

$$J\dot{\omega}_m + B\omega_m + T_L = T_e \quad (1)$$

where  $J$  and  $B$  are the inertia constant and the viscous friction coefficient of the induction motor respectively;  $T_m$  is the external load,  $\omega_m$  is the rotor mechanical speed in terms of angular frequency, which is related to the rotor electrical speed by the expression  $\omega_m = 2\omega_r/p$ , where  $p$  is the number of poles, and  $T_e$  denotes the torque generated by the induction motor defined as (see [1]):

$$T_e = \frac{3p}{4} \frac{L_m}{L_r} (\Psi_{dr}^e i_{qs}^e - \Psi_{qr}^e i_{ds}^e) \quad (2)$$

where  $\Psi_{dr}^e$  and  $\Psi_{qr}^e$  are the rotor flux linkages, with the superscript 'e' denoting that the parameter is referred to the synchronously rotating reference frame;  $i_{ds}^e$  and  $i_{qs}^e$  are the stator current torque and flux components,  $L_r$  is the rotor inductance,  $L_m$  is the magnetizing inductance and  $p$  represents the pole numbers as above. The relation between this synchronous rotating reference frame ( $d^e-q^e$ ) and the three-phase ( $a-b-c$ ) stationary reference frame is given by the so-called reverse Park's transformation (see [12]):

$$\begin{bmatrix} x_a \\ x_b \\ x_c \end{bmatrix} = \begin{bmatrix} \cos(\theta_e) & -\sin(\theta_e) \\ \cos(\theta_e - 2\pi/3) & -\sin(\theta_e - 2\pi/3) \\ \cos(\theta_e + 2\pi/3) & -\sin(\theta_e + 2\pi/3) \end{bmatrix} \begin{bmatrix} x_d \\ x_q \end{bmatrix} \quad (3)$$

where  $\theta_e$  is the angle position between the d-axis of the synchronously rotating reference frame and the a-axis of the stationary reference frame, assuming that the quantities are balanced. And so that  $\hat{\theta}_e$  represents the estimated angular position of the rotor flux vector ( $\bar{\psi}_r$ ) related to the a-axis of the three-phase reference frame. At this point, note that the stationary reference frame axis ( $d^e-q^e$ ) may be considered as a particular case of frame ( $d^e-q^e$ ) where the above angular position becomes zero. Therefore, the mentioned relation (3) is also valid for the ( $d^e-q^e$ )  $\rightarrow$  ( $a-b-c$ ) axis transformation.

Then, using the field orientation control principle (see, for instance [1], [2] and [3]), the current component  $i_{ds}^e$  may be aligned in the direction of the rotor flux vector  $\bar{\psi}_r$ , and the current component  $i_{qs}^e$  may be aligned in the direction perpendicular to it. Under this conditions, it is satisfied that:

$$\Psi_{qr}^e = 0, \quad \Psi_{dr}^e = |\bar{\psi}_r| \quad (4)$$

Taking in account these expressions resulting from the above convenient field orientation, the equation of an induction motor (2) may be simplified to:

$$T_e = \frac{3p}{4} \frac{L_m}{L_r} \Psi_{dr}^e i_{qs}^e = K_T i_{qs}^e \quad (5)$$

where  $K_T$  represents the torque constant, and may be defined as:

$$K_T = \frac{3p}{4} \frac{L_m}{L_r} \Psi_{dr}^{e*} \quad (6)$$

where  $\Psi_{dr}^{e*}$  denotes the command rotor flux.

Also, using the above mentioned field orientation, the dynamics of the rotor flux comes given by (see [1]):

$$\frac{d\Psi_{dr}^e}{dt} + \frac{\Psi_{dr}^e}{T_r} = \frac{L_m}{T_r} i_{ds}^e \quad (7)$$

with  $T_r = \frac{L_r}{R_r}$  being the rotor time constant.

And then, the mechanical equation (1) may be rewritten as:

$$\dot{\omega}_m + a\omega_m + f = b i_{ds}^e \quad (8)$$

being:  $a = B/J$ ;  $b = K_T/J$  and  $f = T_L/J$ .

## 2.2. Implementation of observed-based DFO Control

Taking into account the above results, the DFO Control scheme can be implemented as indicated in Fig. 1 (see [3] and [13]), where the induction motor is commanded by a current-controlled PWM inverter. The functions of the blocks that appear in this figure are the following:

The block 'Speed Tracking Controller' represents the chosen controller to be used to follow the desired angular speed reference  $\omega_r^*$  with the help of the mechanical model presented in Section 2.1. The blocks ' $i_{qs}^{e*}$

Calculation' and ' $i_{ds}^{e*}$  Calculation' implement the necessary calculations to obtain the corresponding flux and torque current component commands using the rotor flux ( $\bar{\psi}_r$ ) value and the unit vector ( $\cos\theta_e$  and  $\sin\theta_e$ ) provided by the inner blocks (see Section 3). The blocks 'dq\*/abc' and 'abc/dq\*' perform the conversion between the synchronously rotating and the stationary reference frames given by Eq. (3). The block 'Current Controller' consists of tree hysteresis-band current PWM control, which is basically and instantaneous feedback current control of PWM where the actual current ( $i_{abc}$ ) continually tracks the command current ( $i_{abc}^*$ ) within a hysteresis band. The block 'Current Regulated PWM Inverter' is a six IGBT-diode bridge inverter with a DC voltage source. The current regulator determines the command signal in the form of digital pulses for the IGBT-diode of the inverter to turn on, so that the current injected in the motor phase depends on the firing angle of this signal. Note that, since the current in an inductive load (the windings of the motor) is proportional to the integral of the voltage applied on it, the current regulator actually controls the time that the DC voltage is applied to the motor phases, and hence, it controls its current. Finally, the block 'Flux Observer' implements the different models for rotor flux estimation that will be

developed in the following sections. These observers will be based on the so-called Voltage or Current Models (see [14] and [15]), so that not all of the inputs of the flux

observer block represented in the general control scheme of Fig. 1 will be considered for each one.

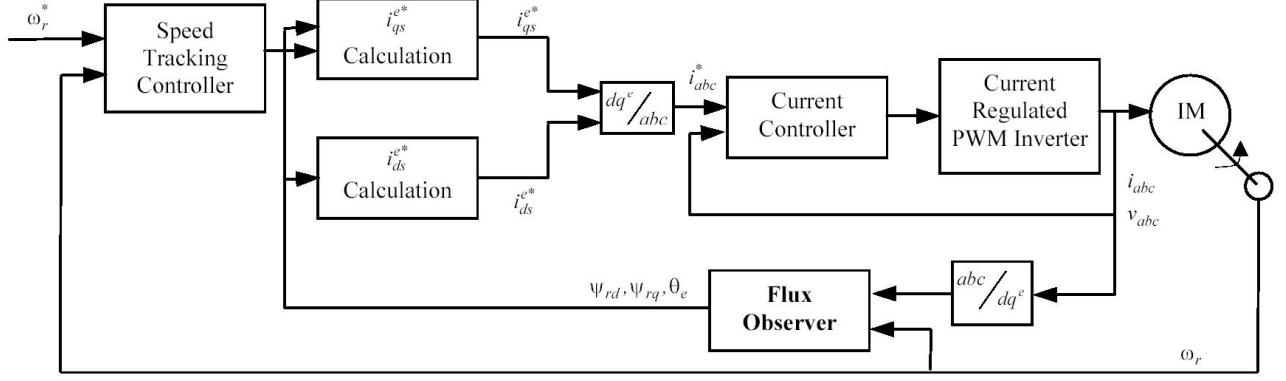


Fig. 1. Block diagram of the proposed DFO control scheme

### 3. Voltage-based Flux Observer Model

In general, the word observer refers to estimators that employ integration process models, and implies essentially a real-time simulation of the physical process at hand, i.e., the induction machine in this work. As indicated, when dealing with DFO Control, the objective is to estimate the rotor flux components. And depending on the system variables utilized for this purpose the structure of the observer varies. In this way, the input variables sensed in the case of the voltage-based flux observer model are the machine terminal voltages and currents.

Let us consider the stationary reference frame ( $d^s$ - $q^s$ ). It is always possible to choose  $q^s$ -axis with the same orientation that the  $a$ -axis of the three-phase reference frame, in such way that the correspondent angle  $\theta = 0$ , and so, applying (3) the following expressions are obtained:

$$i_{qs}^s = i_a; \quad i_{ds}^s = -\frac{1}{\sqrt{3}}(i_a + 2i_b) \quad (9)$$

$$v_{ds}^s = \frac{1}{3}(v_{ab} + v_{ac}); \quad v_{qs}^s = -\frac{1}{\sqrt{3}}v_{bc} \quad (10)$$

where  $i_{qs}^s, i_{ds}^s, v_{ds}^s, v_{qs}^s$  are the flux and torque components of the currents and voltages referred to the above mentioned stationary reference frame and expressed in terms of the sensed three-phase currents and voltages.

On the other hand, considering the dynamical model of the induction machine (see [1] and [2]) one has that the stator flux components referred to the stationary reference frame are given by:

$$\psi_{ds}^s = \int (v_{ds}^s - R_s i_{ds}^s) dt \quad (11)$$

$$\psi_{qs}^s = \int (v_{qs}^s - R_s i_{qs}^s) dt \quad (12)$$

where  $R_s$  is the stator resistance.

Besides, the air gap flux linkage is defined as:

$$\psi_{dm}^s = L_m(i_{ds}^s + i_{dr}^s) = \psi_{ds}^s - L_{ls}i_{ds}^s \quad (13)$$

$$\psi_{qm}^s = L_m(i_{qs}^s + i_{qr}^s) = \psi_{qs}^s - L_{ls}i_{qs}^s \quad (14)$$

where  $L_{ls}$  represents the stator leakage inductance, and the rotor flux may be expressed as:

$$\psi_{dr}^s = L_m i_{ds}^s + L_r i_{dr}^s \quad (15)$$

$$\psi_{qr}^s = L_m i_{qs}^s + L_r i_{qr}^s \quad (16)$$

Finally, eliminating  $i_{dr}^s$  and  $i_{qr}^s$  in the above equations using Eqs. (13-14), and substituting  $\psi_{dm}^s$  and  $\psi_{qm}^s$  in the resulting expressions, it is obtained that:

$$\psi_{dr}^s = \frac{L_r}{L_m}(\psi_{ds}^s - \sigma L_s i_{ds}^s) \quad (17)$$

$$\psi_{qr}^s = \frac{L_r}{L_m}(\psi_{qs}^s - \sigma L_s i_{qs}^s) \quad (18)$$

with  $L_s$  being the stator inductance,  $\sigma = 1 - \frac{L_m^2}{L_r L_s}$  and

where  $i_{ds}^s, i_{qs}^s$  are available from (9) and  $\psi_{dr}^s, \psi_{qr}^s$  are available by means of (11-12) and then from (10).

### 4. Current-based Flux Observer Model

In this case, the input variables to be sensed are the currents and the rotor speed. In the same way that above, the stator flux components of the induction machine dynamical model, referred to the stationary reference frame may be expressed in terms of those variables:

$$\frac{d\psi_{dr}^s}{dt} + R_r i_{dr}^s - \omega_r \psi_{qr}^s = 0 \quad (19)$$

$$\frac{d\psi_{qr}^s}{dt} + R_r i_{qr}^s - \omega_r \psi_{dr}^s = 0 \quad (20)$$

Then, operating with Eqs. (15-16) it is obtained that:

$$\frac{d\psi_{dr}^s}{dt} = \frac{L_m}{T_r} i_{ds}^s - \omega_r \psi_{qr}^s - \frac{1}{T_r} \psi_{dr}^s \quad (21)$$

$$\frac{d\psi_{qr}^s}{dt} = \frac{L_m}{T_r} i_{qs}^s - \omega_r \psi_{dr}^s - \frac{1}{T_r} \psi_{qr}^s \quad (22)$$

where  $\omega_r$  is directly available and where  $i_{ds}^s$ ,  $i_{qs}^s$  are available from (9).

## 5. Simulation Results

In this section, the two above model-based flux observers are compared when implemented within the DFO control scheme proposed in Fig. 1. The induction machine drive used for both case studies is a 50HP, 460Volt, four pole, 60Hz motor with the following parameter specifications:

$R_r=0.228\Omega$ ,  $R_s=0.087\Omega$ ,  $L_r=35.5\text{mH}$ ,  $L_s=35.5\text{mH}$  and  $L_m=34.7\text{mH}$ . Besides, the system has the following mechanical parameters:  $J=1.662\text{kg}\cdot\text{m}^2$  and  $B=0.1\text{N}\cdot\text{m}\cdot\text{s}$ . In addition, the following values have been chosen for the speed tracking controller:  $K_p=50$ ,  $K_i=100$ .

In order to analyze the simulation results, it is convenient to take into account previously some considerations about the performance of both models: In the case of the current-based flux observer, it may be observed that the influence of parameter estimate errors on the accuracy of the estimated flux is evident from Eqs. (21-22). This accuracy depends on the magnetizing inductance  $L_m$  and mainly on the rotor resistance term  $R_r$  of the rotor time constant (see (7)), which may present a considerable temperature dependence. Although a through parameter sensitivity analysis is beyond the scope of this paper, proofs over the estimated rotor flux show that it is relative unaffected by the rotor inductance.

In contrast with the current-based flux observer, the accuracy of the voltage-based flux observer is not dependent at all on the rotor resistance, but it is very sensitive to the estimates of the inductances  $L_r$ ,  $L_s$ ,  $L_m$  (see (17-18)) and primarily, to the stator resistance  $R_s$  by means of (11-12) which, as in the case of the rotor resistance, depends the temperature. This sensitivity to the stator resistance is particularly noticeable at low frequency because of the low values of the voltage signals  $v_{ds}^s$  and  $v_{qs}^s$ . Besides, the dc offset affects negatively the integration process. However, at higher speed, voltage signal terms become more dominant and the control sensitivity to parametrical errors or parameter variation can be overcome.

In this example, it is desired the rotor speed to follow a low speed command that accelerates until 12 rad/s. The system starts with an initial load torque  $T_L=50\text{N}\cdot\text{m}$ , and at time  $t=2\text{s}$  the load torque steps from this value to  $T_L=100\text{N}\cdot\text{m}$ .

Figure 2 shows the command rotor speed (dashed line) and the real rotor speed for the case of the current-based flux observer. As it may be observed, the rotor speed presents a good performance and tracks the desired speed. Moreover, the speed tracking is slightly affected when the load torque is doubled at time  $t=2\text{s}$ .

Same results are shown in Fig. 3 for the voltage-based flux observer. In this case, it may be observed how the speed tracking, as well as the motor torque shown in Figure 7, being also accurate, are quite more erratic due to above mentioned low speed problems. These low speed problems compose the main limitation of this model.

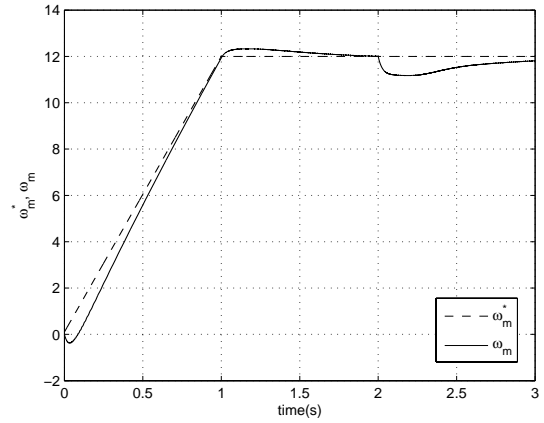


Fig. 2. Reference and real rotor speed signals (rad/s) for the current-based flux observer

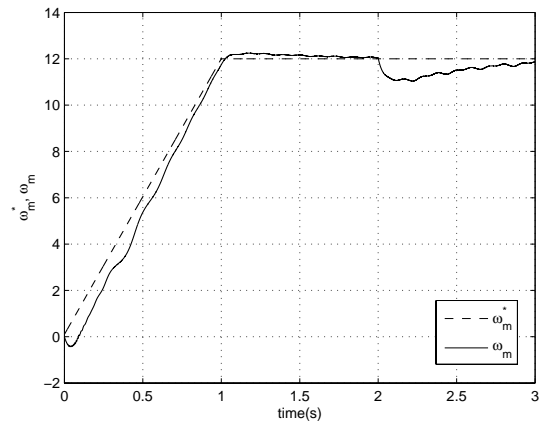


Fig. 3. Reference and real rotor speed signals (rad/s) for the voltage-based flux observer

Figure 4 shows the currents of the stator windings corresponding to the current-based flux observer. It is seen that in the initial estate, the current signals present a high value due to the need of a high torque to increment the rotor speed. In the constant region, the rotor torque has only to compensate the friction and the load torque and consequently, the currents are lower. Finally, at time  $t=2s$  the currents values increase because the load torque has been also increased.

In Fig. 6, the current-based flux observer motor torque evolution is presented. As in the case of the stator currents, the motor torque shows a high initial value in the acceleration zone, then the value decreases until the constant final speed is reached, increases again due to the load torque increment and finally remains constant.

Analogous results for the stator currents and motor torque corresponding to the voltage-based flux observer are shown in Figures 5 and 7, respectively.

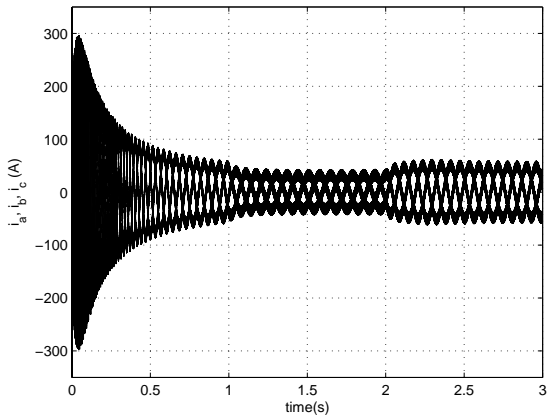


Fig. 4. Stator currents  $i_{abc}(A)$  for the current-based flux observer

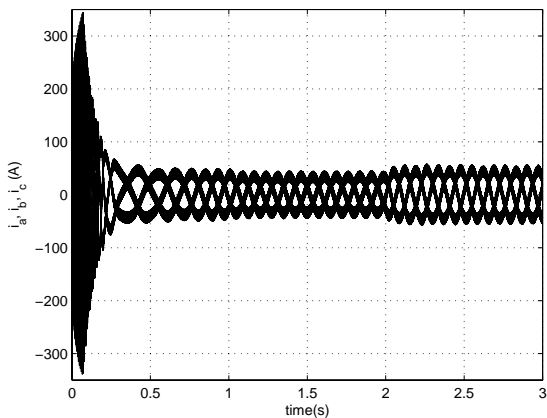


Fig. 5. Stator currents  $i_{abc}(A)$  for the voltage-based flux observer

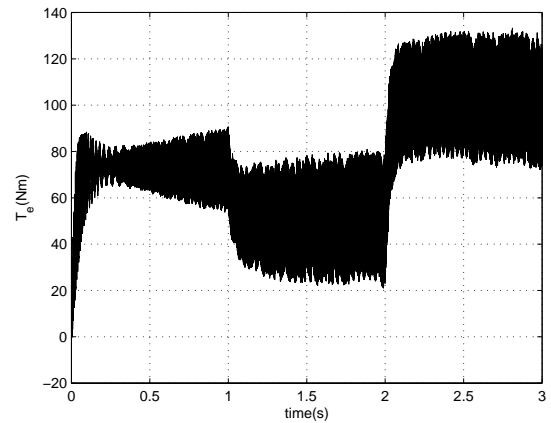


Fig. 6. Motor torque  $T_e(N\cdot m)$  for the current-based flux observer

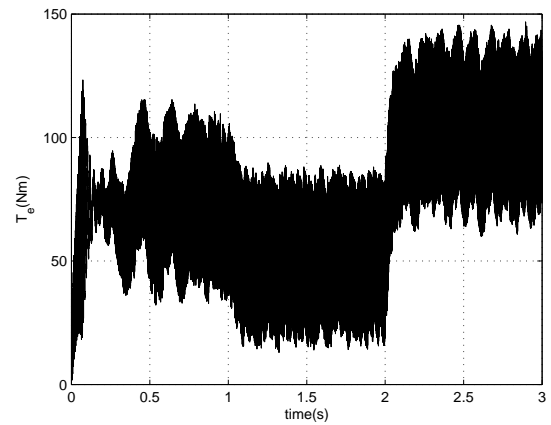


Fig. 7. Motor torque  $T_e(N\cdot m)$  for the voltage-based flux observer

Similar results are obtained for a higher speed command. In the following example it has been used a speed command that accelerates until 120rad/s, with the same load torque step at time  $t=2s$ . Both current-based and voltage-based flux observers present a good performance in terms of stator currents and motor torque, as it may be seen in observed in Figures 10, 11 and 12, 13, respectively. Besides, it may be observed in Figs. 8 and 9 how the trajectory tracking is in this case very similar for both models once overcome the low speed handicap of the voltage-based flux model.

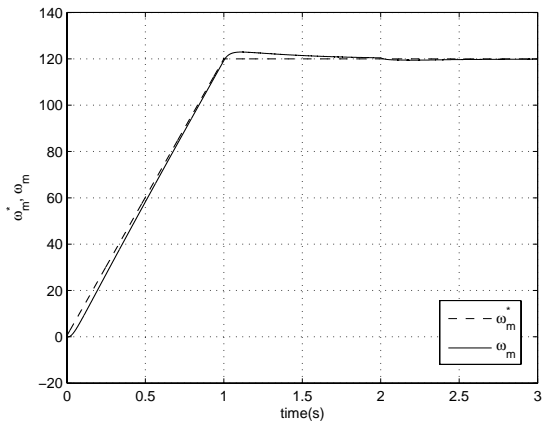


Fig. 8. Reference and real rotor speed signals (rad/s) for the current-based flux observer

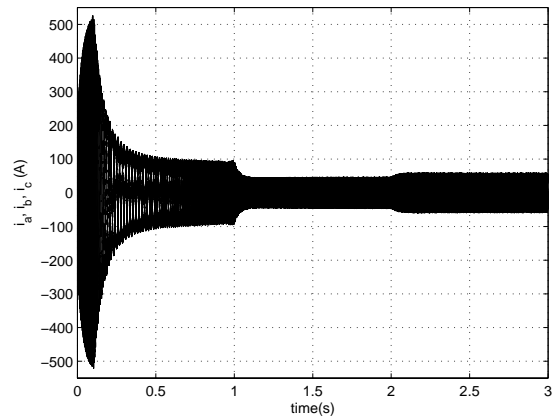


Fig. 11. Stator currents  $i_{abc}$ (A) for the voltage-based flux observer

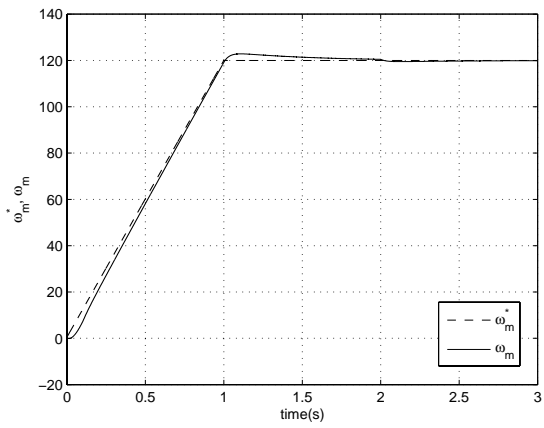


Fig. 9. Reference and real rotor speed signals (rad/s) for the voltage-based flux observer

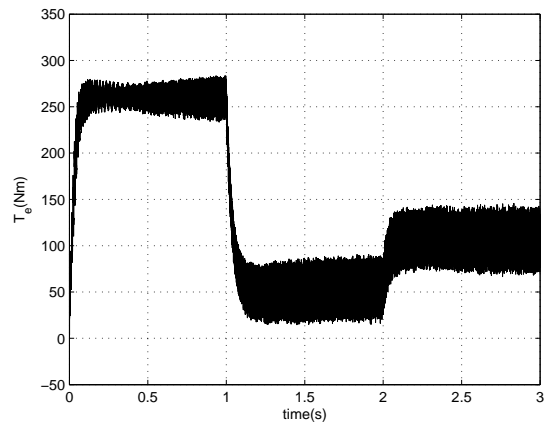


Fig. 12. Motor torque  $T_e$ (N·m) for the current-based flux observer

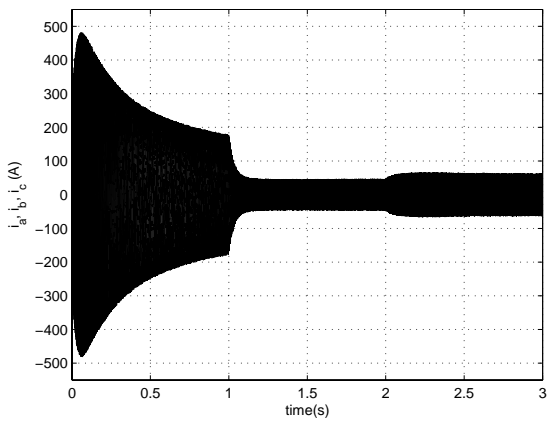


Fig. 10. Stator currents  $i_{abc}$ (A) for the current-based flux observer

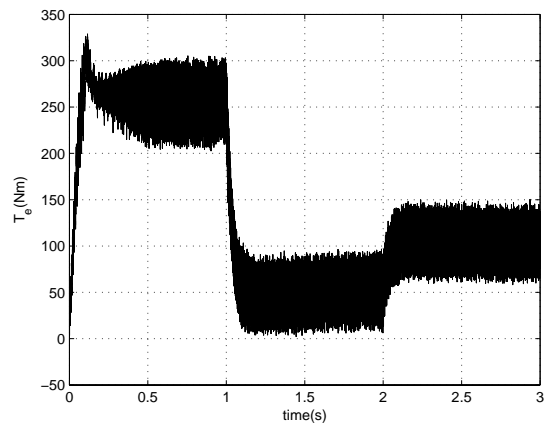


Fig. 13. Motor torque  $T_e$ (N·m) for the voltage-based flux observer

## 6. Conclusion

In this paper two different observer-based flux estimators for direct field orientation has been developed and then analyzed and compared when applied to the control of induction machines. The observers present a different behavior because of the nature of the input variables considered for each one, and they may be classified as current-based or voltage-based models depending on the choice of these inputs.

It has been provided a performance analysis and comparison of both flux observers when applied to the speed tracking problem of a piecewise loaded induction motor drive. As conclusion, it has been shown that the current-based flux observer presents a better performance at low speed due to the low frequency problems of the voltage-based flux model, while affording a similar performance at high speed. Nevertheless, it has to be taken into account that the sensitivity to parametrical errors or parameter variation of the voltage-based model decreases at high frequency, while the current-based sensitivity remains. And note also that a flux vector estimation error due to an incorrect orientation in the DFO control system is equivalent to the presence of motor parametrical errors. Therefore, it would be desirable to combine both estimation models in order to achieve the good performance of the current-based flux observer at low frequencies and the behaviour of the voltage-model at high frequencies.

## Acknowledgements

The authors are very grateful to UPV/EHU by the support of this work through the research project 1/UPV 00146.363-E-16001/2004. They are also grateful to UPV/EHU and DGES by its partial support through projects 9/UPV 00106.I06-15263/2003 and DPI2003-0164 respectively.

## References

- [1] Bose, B.K., *Modern Power Electronics and AC Drives*, Prentice Hall, New Jersey, 2001.
- [2] Vas, P., *Vector Control of AC Machines*, Oxford University Press, Oxford, 1996.
- [3] Novotny D.W., *Vector Control and Dynamics of AC Drives*, Oxford University Press, Oxford, 1996.
- [4] Gan, W.C. and Qiu, L. Design and Analysis of a Plug-in Robust Compensator: An Application to Indirect Field-Oriented Control Induction Machine Drives. *IEEE Trans. on Industrial Electronics*, vol. 50, no. 2, pp. 272-282, 2003.
- [5] Huang, M.S. and Liaw, C.M. Improved Field-Weakening Control for IFO Induction Motor. *IEEE Transactions on Aerospace and Electronic Systems*, vol. 39, no. 2, pp. 647-659, 2003.
- [6] Chern, T., Chang, J. and Tsai, K. Integral-variable-structure-control-based adaptive speed estimator and resistance identifier for an induction motor. *Int. J. Control*, vol. 69, no. 1. pp. 31-47. 1998.
- [7] Barambones, O. and Garrido, A.J. A sensorless variable structure control of induction motor drives. *Electric Power Systems Research*, no. 72, pp. 21-32, 2004.
- [8] Gan, W.C. and Qiu, L. A gain scheduled robust regulator for torque ripple elimination of AC permanent motor systems. *Proc. of IEEE International Conference on Control Applications (CCA04)*. pp. 284-289, Taiwan, 2004.
- [9] Vas, P. *Sensorless Vector and Direct Torque Control*. Oxford University Press, Oxford, 1998.
- [10] Kreindler, L., Moreira, J.C., Testa, A. and Lipo, T.A. Direct field orientation controller using the stator phase voltage third harmonic. *IEEE Trans. on Industry Applications*, vol. 30, no. 2, pp. 441-447, 1994.
- [11] Shen, J.X., Zhu, Z.Q. and Howe, D. Sensorless Flux-Weakening Control of Permanent-Magnet Brushless Machines Using Third Harmonic Back EMF. *IEEE Trans. on Industry Applications*, vol. 40, no. 6, pp. 1629-1636, 2004.
- [12] Texas Instruments. Clarke and Park transforms. *T.I. Reports*, literature number BPRA048, 1998.
- [13] Rehman, H.U. Elimination of the Stator Resistance Sensitivity and Voltage Sensor Requirement Problems for DFO Control of an Induction Machine. *IEEE Trans. on Industrial Electronic*, vol. 52, no. 1, pp. 263- 269, 2005.
- [14] Hinkkanen M. and Luomi J. Modified integrator for voltage model flux estimation of induction motors. *IEEE Transactions on Industrial Electronics*, vol. 50, no. 4, pp. 818-820. 2003.
- [15] Rehman, H.U., Gilven, M.K., Derdiyok, A. and Longya, X. A new current model flux observer insensitive to rotor time constant and rotor speed for DFO control of induction machine. *Proc. of the 32nd IEEE Annual Power Electronics Specialists Conference (PESC01)*. pp. 1179-1184, Vancouver, 2001.